

Fingerprinting Hysteresis

Helmut G. Katzgraber^a, Gary Friedman^b, and G. T. Zimányi^c

^a*Theoretische Physik, ETH Hönggerberg, CH-8093 Zürich, Switzerland**

^b*Drexel University, ECE Department, Magnetic Microsystems Laboratory, Philadelphia, PA 19104 and*

^c*Department of Physics, University of California, Davis, California 95616*

(Dated: November 22, 2013)

We test the predictive power of first-order reversal curve (FORC) diagrams using simulations of random magnets. In particular, we compute a histogram of the switching fields of the underlying microscopic switching units along the major hysteresis loop, and compare to the corresponding FORC diagram. We find qualitative agreement between the switching-field histogram and the FORC diagram, yet differences are noticeable. We discuss possible sources for these differences and present results for frustrated systems where the discrepancies are more pronounced.

Keywords: spin glasses, first-order reversal curves, switching-field histograms

INTRODUCTION

The conventional methods [1, 2, 3] to characterize magnetic interactions in hysteretic systems, such as the δM method [4, 5], utilize isothermal remanent magnetization (IRM) and dc demagnetization remanence (DCD) curves based on the Wohlfarth relation [6]. Recently, FORC diagrams [7, 8] have been introduced to study hysteretic systems. Their extreme sensitivity has helped to “fingerprint” several experimental systems as well as theoretical models ranging from geological samples and recording media to paradigmatic models of random magnets and spin glasses [8].

In this work we perform numerical simulations of random magnets (and spin glasses) in order to test the predictive power of FORC diagrams by comparing to a histogram of up- and down-switching fields of the underlying switching units along the major hysteresis loop.

The aforementioned re-parametrization of the major hysteresis loop (switching-field histogram) displays the information carried by the major loop in a more comprehensive way and provides a good comparison to the FORC diagram. We find, that the major-loop behavior predicts the minor-loop behavior captured by FORC diagrams well. We present a comparison of both distributions and discuss some differences between them. We argue that switching-field histograms are useful to study hysteretic systems in more detail than with conventional methods due to their simplicity and ease to compute.

MODEL & ALGORITHM

The Hamiltonian of the random-field Ising model (RFIM) is given by [9]

$$\mathcal{H} = \sum_{\langle i,j \rangle} J_{ij} S_i S_j - \sum_i h_i S_i - H \sum_i S_i. \quad (1)$$

Here $S_i = \pm 1$ are Ising spins on a square lattice of size $N = L^3$ in three dimensions with periodic boundary conditions. The interactions between the spins are uniform

($J_{ij} = 1$) and nearest-neighbor, and H represents the externally applied field. Disorder is introduced into the model by coupling the spins to site-dependent random fields h_i drawn from a Gaussian distribution with zero mean and standard deviation σ_R .

We simulate the zero-temperature dynamics of the RFIM by changing the external field H in small steps starting from positive saturation. After each field step we compute the local field f_i of each spin:

$$f_i = \sum_j J_{ij} S_j - H - h_i. \quad (2)$$

A spin is unstable if it points opposite to its local field, i.e., $f_i \cdot S_i < 0$. We then flip a randomly chosen unstable spin and update the local fields at neighboring sites. This procedure is repeated until all spins are stable.

For the rest of this work we set $L = 50$ ($N = 125000$ spins) and $\sigma_R = 5.0$, unless otherwise specified. The different figures are calculated by averaging over 5000 disorder realizations in order to reduce finite-size effects.

FORC DIAGRAMS

In order to calculate an FORC diagram, a family of First Order Reversal Curves (FORCs) with different reversal fields H_R is measured, with $M(H, H_R)$ denoting the resulting magnetization as a function of the applied and reversal fields. Computing the mixed second order derivative [7, 10]

$$\rho(H, H_R) = -\frac{1}{2} [\partial^2 M / \partial H \partial H_R] \quad (3)$$

and changing variables to $H_c = (H - H_R)/2$ and $H_b = (H + H_R)/2$, the local coercivity and bias respectively, yields the “FORC distribution” $\rho(H_b, H_c)$. FORC diagrams resemble the commonly known Preisach diagrams [11, 12], yet they are model-independent and therefore more general.

Figure 1 shows an FORC diagram of the RFIM at high disorder strength ($\sigma_R = 5.0 > \sigma_{\text{crit}} \approx 2.16$) [13].

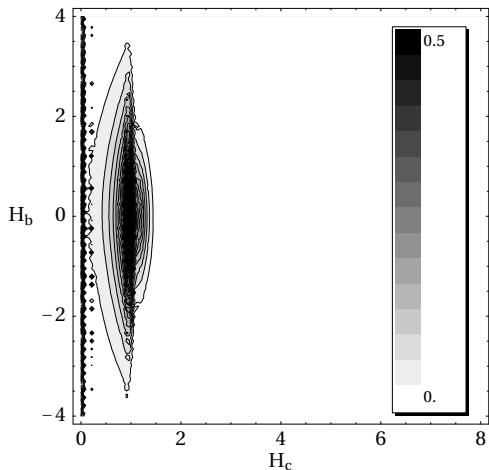


FIG. 1: FORC diagram of the RFIM for disorder $\sigma_R = 5.0$, well above the critical disorder [13] in three dimensions. Note the pronounced vertical feature at $H_c = 1$ with a wake extending to $H_c = 0$ which corresponds to multi-domain nucleation in the sample. The dots along the H_b -axis are numerical noise (no data smoothing).

Note the vertical ridge at $H_c \approx 1$ reminiscent of domain-wall nucleation [14]. A vertical cross-section of the ridge ($H_c = 1$) mirrors the distribution of the applied random fields, because these can be viewed as a distribution of random biases acting on the spins when $\sigma_R \gg \sigma_{\text{crit}}$. We have tested this in detail by selecting the random fields from a box distribution. The resulting FORC diagram is qualitatively similar to the Gaussian case, yet a vertical cross-section of the ridge is box-shaped. This is not evident by studying the major hysteresis loop for different disorder-distribution shapes and illustrates the advantages of the FORC method over conventional approaches for studying hysteretic systems.

SWITCHING-FIELD HISTOGRAMS

In order to test the predictive power of FORC diagrams, we simulate the RFIM with the zero-temperature dynamics described in Sec. and store the up- and down-switching fields of the spins along the major hysteresis loop. We then create a histogram of the number of flipped spins for a given pair of up- (H_\uparrow) and down-switching fields (H_\downarrow). By changing the variables to the coercivity [$H_c = (H_\uparrow - H_\downarrow)/2$] and bias [$H_b = (H_\uparrow + H_\downarrow)/2$] of each spin, we obtain a distribution of the coercivities and biases of the spins in the system along the major hysteresis loop.

Figure 2 shows the switching-field histogram (SFH) for the RFIM. One can see a close resemblance with the corresponding FORC diagram presented in Fig. 1. In order to better compare FORC diagram and SFH, in Fig. 3 we

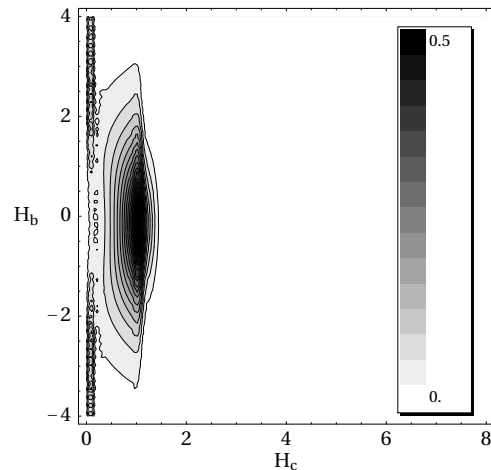


FIG. 2: Switching-field histogram of the three-dimensional RFIM with $\sigma_R = 5.0$. Note the close resemblance to the FORC diagram presented in Fig. 1. Because no derivatives of the data are required, the contours are much smoother than in the case of an FORC diagram.

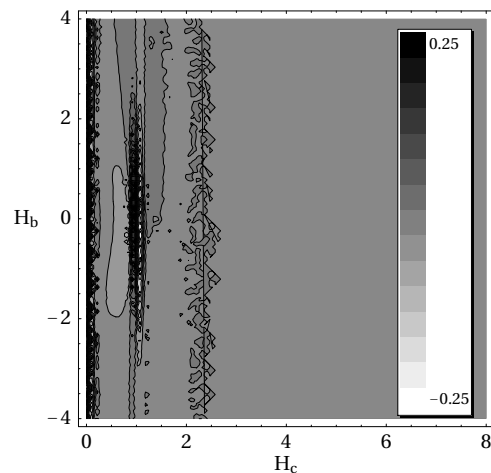


FIG. 3: Absolute difference between the FORC diagram presented in Fig. 1 and the corresponding SFH in Fig. 2 for the three-dimensional RFIM with $\sigma_R = 5.0$. The details are discussed in the text.

present the absolute difference between both diagrams.

Even though the SFH and the FORC diagram of the RFIM differ slightly (see Fig. 3), the main characteristics representing the underlying physical properties of the model are the same (vertical ridge representing multi-domain nucleation). It is interesting that a zeroth-order reversal curve (the major hysteresis loop) contains possibly all the necessary information to reconstruct the first order reversal curves of the system (the FORC diagram).

The differences found between the FORC diagram and the SFH could be due to numerical error in the derivatives of the FORCs because noise is amplified in numer-

ical derivatives considerably. In addition, the differences could be attributed to either hysteron correlations or the failure of the (simple) Preisach picture of hysterons. The latter would imply that a generalization of “classical” hysterons is required.

Figure 2 also illustrates how the re-parametrization of the major hysteresis loop in terms of an SFH shows more details about the microscopic structure of the system. The gained information is similar to the information provided by an FORC diagram, yet the computation of an SFH is *considerably* faster than calculating an FORC diagrams (generally $\sim 10^2$ times faster) and involves no numerical derivatives of the data, thus reducing numerical error.

FRUSTRATED SYSTEMS

As the random-field Ising model is a random magnet with no frustration, we also calculate the FORC diagram and SFH for the 3D Edwards-Anderson Ising spin glass [15] (EASG). Due to frustration, a spin can flip more than twice along the full hysteresis loop. With the current definition of the SFH this is not taken into account and differences to an FORC diagram are expected.

The Hamiltonian of the Edwards-Anderson Ising spin glass is given by Eq. (1) where the J_{ij} are nearest-neighbor interactions chosen according to a Gaussian distribution with zero mean and standard deviation unity, and $h_i = 0 \forall i$. H represents the externally applied magnetic field and periodic boundary conditions are applied. For the simulations we use the zero-temperature algorithm presented in Sec. . Frustration is introduced by the random signs of the interactions J_{ij} .

Figure 4 shows the FORC diagram of the EASG. One can see a pronounced ridge along the H_c -axis together with an asymmetric feature at small coercivities. The underlying details of the EASG FORC diagram have been discussed elsewhere [8].

In Fig. 5 the SFH of the EASG is shown. Note that the asymmetry present in the FORC diagram in Fig. 4 is lost. The weight of the asymmetric part of the FORC diagram shifts to the ridge at $H_b = 0$.

Although some of the features in the FORC diagram (Fig. 4) of the EASG are missing in the corresponding SFH (Fig. 5), the horizontal ridge reminiscent of the underlying reversal-symmetry of the Hamiltonian [8] is conserved. In particular, by comparing the FORC diagram and SFH one can study the effects of frustration on the hysteretic behavior of a spin glass.

CONCLUSIONS

By re-parameterizing the major hysteresis loop with a switching-field histogram we show that for systems with

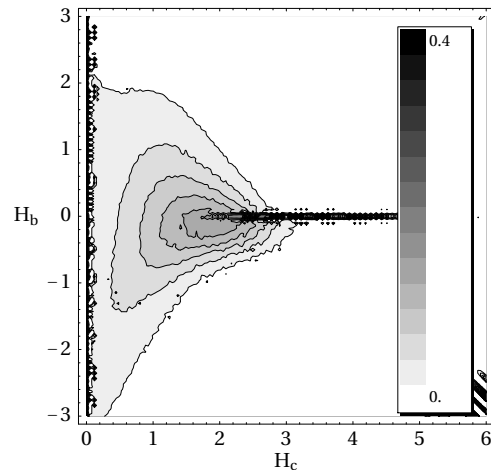


FIG. 4: FORC Diagram of the EASG. Note the ridge along the H_c -axis. Data for 5000 disorder realizations and $N = 50^3$ spins.

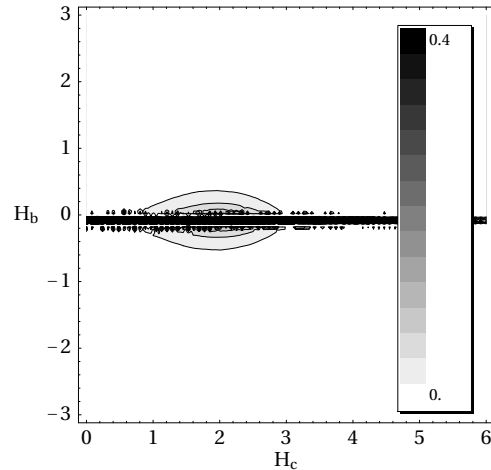


FIG. 5: SFH of the EASG. While the ridge along the H_c -axis is qualitatively conserved, the SFH shows drastic differences to the FORC diagram presented in Fig. 4. In particular, the asymmetry with respect to the horizontal axis is lost.

no frustration (random-field Ising model) the SFH closely resembles the FORC diagram. Small differences can be attributed to numerical error in the calculation of an FORC diagram, hysteron correlations, or the breakdown of the hysteron picture.

SFHs show more details about the system than the major hysteresis loop and are considerably faster to compute than FORC diagrams. Therefore they are an efficient alternative in order to study the microscopic distributions of coercivity and bias of the switching units.

Because the switching fields of the underlying microscopic switching units have to be recorded for the computation of an SFH, the method is in general limited to numerical studies of hysteretic systems. Experimental

applicability might be possible with synthetic particulate samples [16] where the individual switching units can be traced during the magnetic field sweep.

We also present results on the (frustrated) Edwards-Anderson Ising spin glass. We show that there are clear differences between the FORC diagram and the SFH because SFHs do not take into account multiple switching events of the spins, a hallmark of spin glasses. We suggest these differences can be used to quantify the effects of frustration in FORC diagrams.

The FORC and SFH methods promise to be powerful tools to “fingerprint” hysteretic systems. Still, the breadth of information they provides remains to be understood fully.

Acknowledgments

We would like to thank F. Pázmándi and R. T. Scalettar for discussions.

* Electronic address: katzgraber@phys.ethz.ch; Fax: +41 1 633 11 15 (author responsible for further correspondence)

[1] X. He, C. Alexander Jr., and M. R. Parker, *IEEE Trans. Magn. MAG-28* p. 2683 (1992).

- [2] R. Proksh and B. Moskowitz, *J. Appl. Phys.* **75**, 5894 (1994).
- [3] P. Hedja, E. Petrovsky, and T. Zelinka, *IEEE Trans. Magn. MAG-30* p. 896 (1994).
- [4] X.-D. Che and H. N. Bertram, *J. Magn. Magn. Mater.* **116**, 131 (1992).
- [5] M. El-Hilo, K. O’Grady, P. I. Mayo, and R. W. Chantrell, *IEEE Trans. Magn. MAG-28* p. 3282 (1992).
- [6] E. P. Wohlfarth, *J. Appl. Phys.* **29**, 595 (1958).
- [7] C. R. Pike, A. P. Roberts, and K. L. Verosub, *J. Appl. Phys.* **85**, 6660 (1999).
- [8] H. G. Katzgraber, F. Pázmándi, C. R. Pike, K. Liu, R. T. Scalettar, K. L. Verosub, and G. T. Zimányi, *Phys. Rev. Lett.* **89**, 257202 (2002).
- [9] H. Ji and M. Robbins, *Phys. Rev. B* **46**, 14519 (1992).
- [10] E. Della Torre, *Magnetic Hysteresis* (IEEE Press, New York, 1999).
- [11] F. Preisach, *Z. Phys.* **94**, 277 (1935).
- [12] I. D. Mayergoyz, *IEEE Trans. Magn. MAG-22* p. 603 (1986).
- [13] O. Perkovic, K. A. Dahmen, and J. P. Sethna, *Phys. Rev. B* **59**, 6106 (1999).
- [14] B. Drossel and K. Dahmen, *Euro. Phys. J. B* **3**, 485 (1998).
- [15] K. Binder and A. P. Young, *Rev. Mod. Phys.* **58**, 801 (1986).
- [16] K. Liu, J. Nogués, C. Leighton, I. V. Roshchin, H. Masuda, K. Nishio, and I. K. Schuller, *Appl. Phys. Lett.* **81**, 4434 (2002).